

Available at [www.sciencedirect.com](http://www.sciencedirect.com)journal homepage: [www.elsevier.com/locate/issn/15375110](http://www.elsevier.com/locate/issn/15375110)

## Research Paper

# High-throughput phenotyping technology for maize roots

T.E. Grift<sup>a,\*</sup>, J. Novais<sup>b</sup>, M. Bohn<sup>b</sup>

<sup>a</sup> Department of Agricultural and Biological Engineering, University of Illinois, Urbana, IL 61801, USA

<sup>b</sup> Department of Crop Sciences, University of Illinois, Urbana, IL 61801, USA

### ARTICLE INFO

#### Article history:

Received 26 February 2011

Received in revised form

30 May 2011

Accepted 2 June 2011

Published online 18 July 2011

This paper describes the development of high-throughput measurement techniques allowing acquisition of phenotypical data describing maize roots. One of a maize root's traits is the level of complexity, which was expressed in a Fractal Dimension (FD) calculated from root images. Another important trait is the Root Top Angle (RTA) that was measured using a new machine vision algorithm. The measurement system consisted of a semi-automated imaging box that provided a highly diffuse lighting scene and allowing imaging of up to 700 roots per day.

The measurement techniques were evaluated using roots recovered from a set of 200 recombinant inbred lines (RILs) derived from a cross between maize inbreds B73 and CML333. B73 and CML333 are known to have different root characteristics and their progeny are expected to show segregation for root traits.

Since standard protocols for the measurement of the two root traits are non-existent, no comparisons could be made. Nevertheless, the data showed that the techniques were capable of confirming significant differences in FD among the two inbred lines and their progeny, as well as measuring variations in RTA that are known for the inbreds and their crosses. In addition, first hypotheses about the inheritance of root complexity (as expressed in the FD) and RTA in maize were derived and tested: initial evidence showed that root complexity is a phenotype probably determined by a multitude of genes with small effects. In contrast, the data indicated that the RTA is additively inherited.

© 2011 IAgrE. Published by Elsevier Ltd. All rights reserved.

## 1. Introduction

The acquisition of genotypic data of plants through DNA sequencing has become an inexpensive, high-throughput procedure: the larger problem is currently obtaining high quality phenotypic data for a large number of genotypes. The focus in phenotyping of maize has been on the above ground part, arguable owing to ease of access and the non-destructive nature of the process. The root structure has had considerably less attention, and even less in a high-throughput sense. It is however imperative that the properties of the plant organ that

is actually in contact with soil are investigated in relation to agronomic performance. To interpret the phenotypic information in a genetic sense using a statistically sound procedure, a large number of plants needs to be evaluated. In addition, to evaluate how root complexity influences, for instance, water uptake and nitrogen use efficiency, response to biotic stresses, and overall plant health, a system is required that can measure root morphological parameters in a standardised high-throughput manner.

Architecture of a biological object according to Lynch (1995) is "The spatial configuration of some complex assemblage of

\* Corresponding author.

E-mail address: [grift@illinois.edu](mailto:grift@illinois.edu) (T.E. Grift).

1537-5110/\$ – see front matter © 2011 IAgrE. Published by Elsevier Ltd. All rights reserved.

doi:10.1016/j.biosystemseng.2011.06.004

subunits, with the implication that the overall configuration has some functional significance". In this paper, a practical realisation is offered to measure the complexity, expressed in the Fractal Dimension (FD), and Root Top Angle (RTA) of maize roots. As a test case, two maize inbreds B73 and CML333, which are known to have differing root morphologies, and a large set of progeny derived from their cross, were selected.

### 1.1. Maize root complexity measurement

In this research, the assumption was made that roots are complex structures without adhering to a definition from the biological domain. However, since fractals are complex structures based on a mathematical definition, and since FD is a proven indicator of the level of complexity, the assumption was made that the FD of an assumed complex object such as a maize root is an indicator of its complexity. The reasoning behind the assumption that maize roots are complex objects that can be regarded fractals, lays in the fact that self-similarity, one of the key characteristics of fractals, is present (Richardson & zu Dohna, 2003; Soethe, Lehmann, & Engels, 2007; Spek & Van Noordwijk, 1994). Mandelbrot (1983) was the first to introduce the concept of FD. Fractals are objects that are irregular, but self-similar at various scales (Eshel, 1998; Mandelbrot, 1983). Besides maize roots, many structures in nature appear fractal-like, such as trees, ferns, snowflakes, clouds, sponges, and mountains.

A considerable amount of work has been done to capture the complexity of root systems using FDs, including morphology analysis (Tatsumi, Yamauchi, & Kono, 1989), growth and architecture of bean seedling roots (Lynch, Johannes, & Beem, 1993), and sorghum root morphology (Masi & Maranville, 1998). Oppelt, Kurth, Dzierzon, Jentschke, and Godbold (2000) used FD to compare the root systems of four fruit tree species from Botswana, and Walk, Van Erp, and Lynch (2004) related the FD to the ability of roots to explore soils. Bohn, Novais, Fonseca, Tuberosa, and Grift (2006) used FD to locate regions in the maize genome involved in the inheritance of the primary root system complexity of maize. Lontoc-Roy et al. (2006) used computer tomography to quantify the complexity of root systems in a three-dimensional space. FD has also been used to study other biological objects, such as seaweeds (Kubler & Dugeon, 1996), sponges (Abraham, 2001), neurons (Fernandez et al., 1994), and fungal mycelia (Mihail, Obert, Bruhn, & Taylor, 1995).

### 1.2. Root Top Angle (RTA) measurement

Hammer et al. (2009) used a quantitative dynamic crop growth model to investigate the effect of canopy and root architecture changes on maize yield trends. They concluded that the root architecture, mainly defined by the root angle of the primary root system, may have had a profound influence on the historical maize yield increases in the Mid-Western USA. Although in the research as described here the secondary root system was studied, the research by Hammer et al. (2009) provided the inspiration to measure the RTA of the secondary root system using a set of root images.

### 1.3. Imaging of biological objects

Image acquisition has been conducted previously using video cameras (Cunningham, Adams, Luxmoore, Post, & DeAngelis, 1989; Ottman & Timm, 1984), optical scanners (Arsenault, Poulcur, Messier, & Guay, 1995; Box, 1996; Kaspar & Ewing, 1997), photographic images (Abraham, 2001; Bohn et al., 2006; Eghball, Settini, Maranville, & Parkhurst, 1993; Masi & Maranville, 1998; Tatsumi et al., 1989), and image transparencies (Nielsen & Lynch, 1994). The challenge whilst studying secondary maize root systems lays in the fact that they represent three-dimensional (3D) structures. It is technically demanding to make *in situ* measurements of this type of structures; however, measurements in two dimensions (2D) can be used to estimate the FD of 3D objects (Nielsen & Lynch, 1994). Nuclear Magnetic Resonance (NMR) technology is available to obtain images of 3D structures and to study their FDs. However, this technology is expensive, cannot be applied in a high-throughput fashion, and, with current equipment, large root systems cannot be analysed (Berntson, 1996).

The objective of this research was to develop high-throughput methods allowing the measurement of maize root traits such as FD as a proxy for root complexity, as well as RTA.

## 2. Materials and methods

To evaluate the performance of the high-throughput phenotyping technologies, they were applied in a large-scale experiment. Maize inbreds B73 and CML333 were used as parental materials in this experiment. B73 is a yellow dent inbred, which belongs to the temperate Stiff Stalk Synthetic heterotic group. CML333 is a white flint inbred, developed at CIMMYT, Mexico, that is adapted to tropical climate conditions. Both inbreds were crossed and a set of 200 individuals from their segregating  $F_2$  population were randomly selected. These individuals were advanced by continuous selfing to produce a set of 200 recombinant inbred lines (RILs). Conventional maize hybrids are produced by crossing two maize inbreds from different heterotic pools to maximise hybrid vigour. Therefore, it is of key importance to evaluate new maize inbreds as hybrids. To accomplish this goal, testcrosses were produced by crossing both parental inbreds B73 and CML333 and their RILs to the same inbred PHZ51. PHZ51 belongs to the non-Stiff Stalk heterotic pool. Testcrosses used in this research, were produced by Dr. Flint-Garcia, USDA-ARS, Columbia, Missouri.

The experimental design was an incomplete block design with 204 entries, *i.e.*, the testcrosses of all 200 RILs and their parental inbreds B73 and CML333 and two commercial hybrids as checks, two replications, 34 incomplete blocks and six entries per block. The complete experiment was planted at the "University of Illinois Research Educational Center" in Urbana, Illinois. The experiment was repeated with a single replication at the Missouri Agricultural Experiment Station of the University of Missouri in Columbia, Missouri. Here, the experimental design included two replications, 34 incomplete blocks and six entries per block. Each plot consisted of a single

row of 4.6 m long with 0.76 m spacing between rows. Plots were composed of 25 plants row<sup>-1</sup> (71,525 plants ha<sup>-1</sup>). Plants were uprooted at the R1 (silking) stage, where the first plant in each row was discarded. In Illinois, the next three consecutive plants and in Missouri the next four consecutive plants were trimmed at the third node and uprooted ensuring that for each plant a cubic volume of 0.3 m by 0.3 m by 0.3 m root core was recovered. A simple time study revealed the following average time requirements per root: digging required 84 s, soaking and cleaning using high-pressure water jets required 210 s, and imaging required 45 s giving a total of 5 min and 39 s per root. These time estimates were acquired in a drummer silty clay loam soil under normal soil conditions, meaning that neither compaction nor drought conditions were present. Each root was labelled with a unique barcode that was used in the analysis software to identify the genotype and field location. In this study, a total of 1932 roots were processed at the Agricultural Engineering farm of the University of Illinois.

### 2.1. Imaging system

Maize roots are intricate structures with abundant detail hidden behind outer root branches. To acquire high quality images from objects like these, proper lighting is essential. The objective was to obtain an even diffused lighting scene, thus reducing the shading effect that outer root branches may have on inner branches. For this purpose, a “soft box” was constructed (Fig. 1). It consists of a box structure with an inner dimension of 61 cm square, by 122 cm tall, made from non-

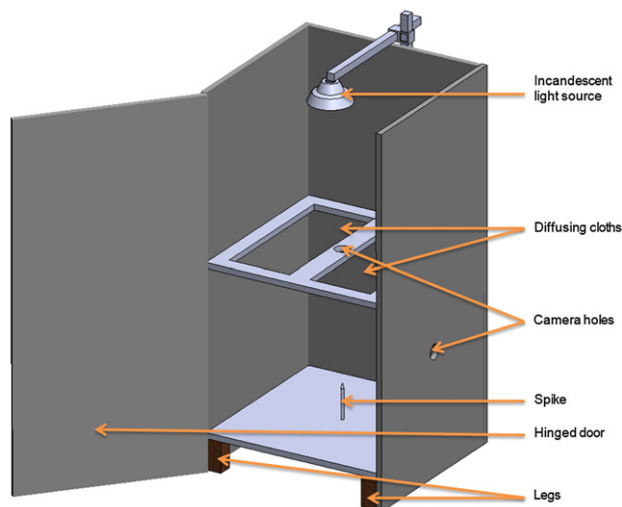


**Fig. 1** – A “soft box” was developed to provide a highly diffuse lighting scene for imaging the intricate structures present in maize roots. The box was made from white non-reflective panel board, with two “shelves”, the upper shelf containing diffusing cloths (made from white sheet material), and a downward looking camera. The bottom shelf contained a spike on which the roots were placed, as well as a mechanism that automatically rotated the root to obtain four perpendicular lateral views from a camera mounted in a side panel. Note that the diffusing cloths are not drawn.

reflective white furniture panels, with two “shelves”. The top shelf contains dual diffusing cloths made from a low-cost white sheet material, (not drawn in the figure). Two monochrome cameras (Unibrain Fire-i 701b), with a maximum resolution of 1280 by 960 pixels were mounted, one in the “bridge” between the diffusing cloths in the top shelf, and another in a side panel to obtain top view and lateral view images. The cameras were fitted with variable focus/variable aperture lenses with a focal length of 6 mm (Pentax C60607KP). The cameras were controlled by a program written in MatLab®, using an IEEE 1394 (FireWire®) interface.

The bottom shelf served as a platform that contains a spike on which the root was pinned upside down, after punching a hole in the stalk. Underneath the spike, a stepper motor was mounted that rotated the root to obtain four lateral images. The stepper motor was controlled by a driver board (model KTA-196, Ocean Controls, Seaford BC, Australia) through a serial connection, under control of the same program that communicated with the cameras. As a light source, a standard photography 250 W incandescent bulb was used. This bulb generated light with such intensity that, under the diffusing cloths no shadow caused by the bridge containing the camera was observed in images. The soft box was fitted with a hinged door for easy frontal access.

In addition to ensuring proper lighting, background subtraction was used to obtain high-contrast images. This was accomplished in software written in MatLab®. Before the operator placed a root in the imaging box, the control program acquired two background images for each root, one from above and one from the side. Subsequently, the operator placed the root on the spike and, after closing the door, one top image and one lateral image were acquired. The machine then automatically rotated the root three times through 90°, so that three more lateral root images were obtained. For analysis, the difference images between the background image and the image containing the root were used. Fig. 2 shows a composite image, where the top two images are originals without background subtraction, and the bottom two images show the effect of background subtraction. It is clear that in the bottom images, the background has vanished, with minimal loss of detail. The left side images show the top views and the right side images show the lateral views of the root. Note that the lateral images are shown upside down, as they were acquired in the imaging box where the root was pinned upside down on the spike.

### 2.2. Fractal dimension as a root complexity indicator

The FD of the roots was determined from the top images as well as the lateral images using the classical “box-counting” method, which was implemented in a MatLab® program. This method consists of applying a fine grid across a binary image and counting the number of pixels that coincide with the root image. Subsequently, the grid size is increased by a factor 2 and the procedure is repeated until the grid size is equal to the image size. Fig. 3 shows this process, with six images, where the resolution is decreased from 256 by 256 pixels to 8 by 8 pixels from top left to bottom right. Each image resulted in a data point that indicated how many pixels in the image coincided with the root image. These points were used to

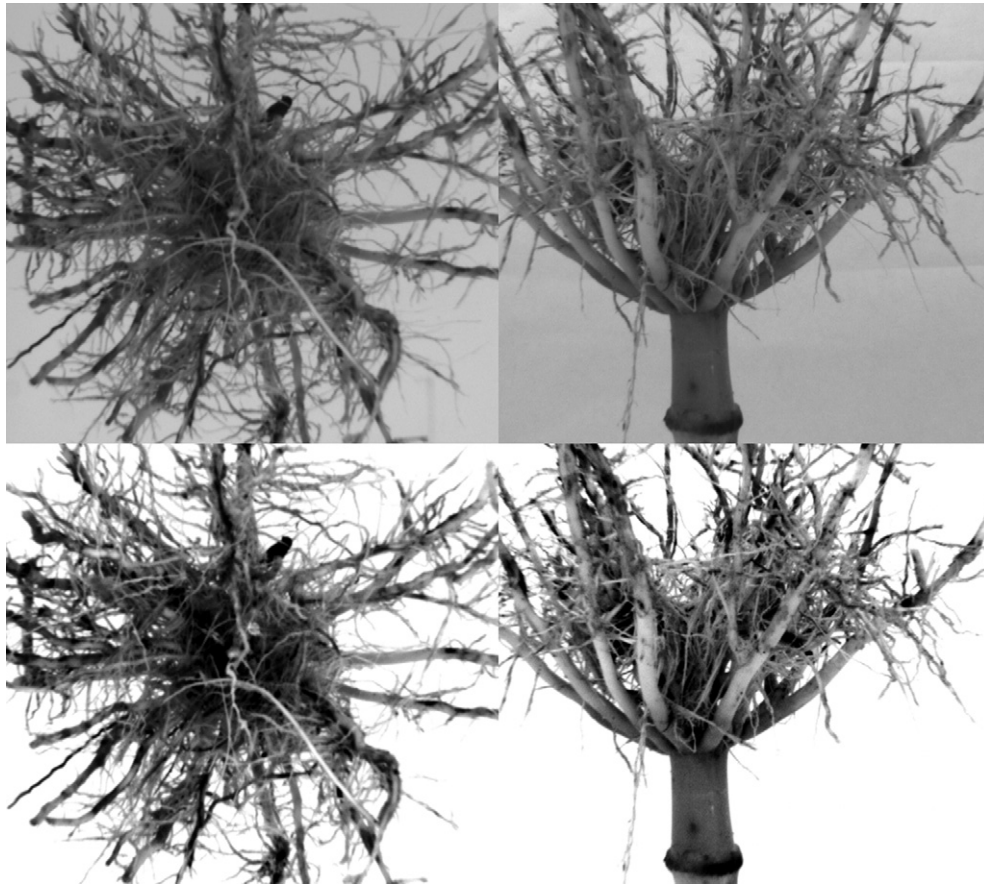


**Fig. 2** – This is a composite image of maize roots. The top images show the originals with the background visible (notice the crevice in the top right image, where the bottom shelf and side panel connect). The bottom images show the roots after background subtraction. Notice that the background has become solid white, even the crevice has been removed, at a low loss of detail.

calculate the FD as the slope of a line in a graph, where the logarithm of the number of intersecting pixels is plotted against the logarithm of the reciprocal value of the grid size. The FD is a continuous variable ranging from one to two for two-dimensional images.

### 2.3. Root Top Angle measurement

The simplest idealised topology of a maize root may be a model where the stalk is approximated by a cylinder and the root section is approximated by a cone (Fig. 4). The challenge is now to determine 1) the starting point of the cylinder at the bottom, which indicates the stalk diameter, 2) the transition point between the cylinder and the cone and 3) the “rim” of the cone.

The process as described here may seem rather trivial at first, but alas, there are many ways in which true roots differ from the ideal topology. To obtain a feel for the difficulty of determining the “correct” root angle, it is a useful exercise to observe the bottom right image in Fig. 2, and try to “estimate” the Left and Right Root Angles. When attempting this, human observers subconsciously separate what is considered root and what is not, what matters and what can be ignored, what is “shape” and what is “texture”. For instance, the smaller vertically oriented branches are typically ignored and an

imaginary straight line is drawn that straddles the larger root branches at the bottom. Some observers may straddle a straight line closer to the stalk than others. The conclusion is simple: a “correct” root angle does not exist, and, therefore, a method was defined that performed consistently for “well behaved roots”, meaning that they have a stalk that can be distinguished, and that the transition point from stalk to root mass is identifiable.

Adopting the ideal topology principle, the following procedure was developed: after converting the monochrome image into a binary image, the first task was to split the image into a left and right hand semi-image to calculate the Left and Right Root Angles independently. For this purpose, the centre of the stalk was required. However, in many images, not only does the stalk intercept the pixel row at the bottom of the image, but often root branches and sometimes brace roots are present in the lowest pixel row. To distinguish the maize stalk from other objects, the lengths of all objects that intersected the lowest pixel row were calculated and the largest contiguous line segment was considered the stalk. To capture the overall “shape” or “mass” of the root, the pixels were accumulated across the complete length of the root (Fig. 5), and the coordinates ( $p_{top}, q_{top}$ ) representing the “rim” of the cone were set as the maximum value of the accumulated pixels along the horizontal axis.

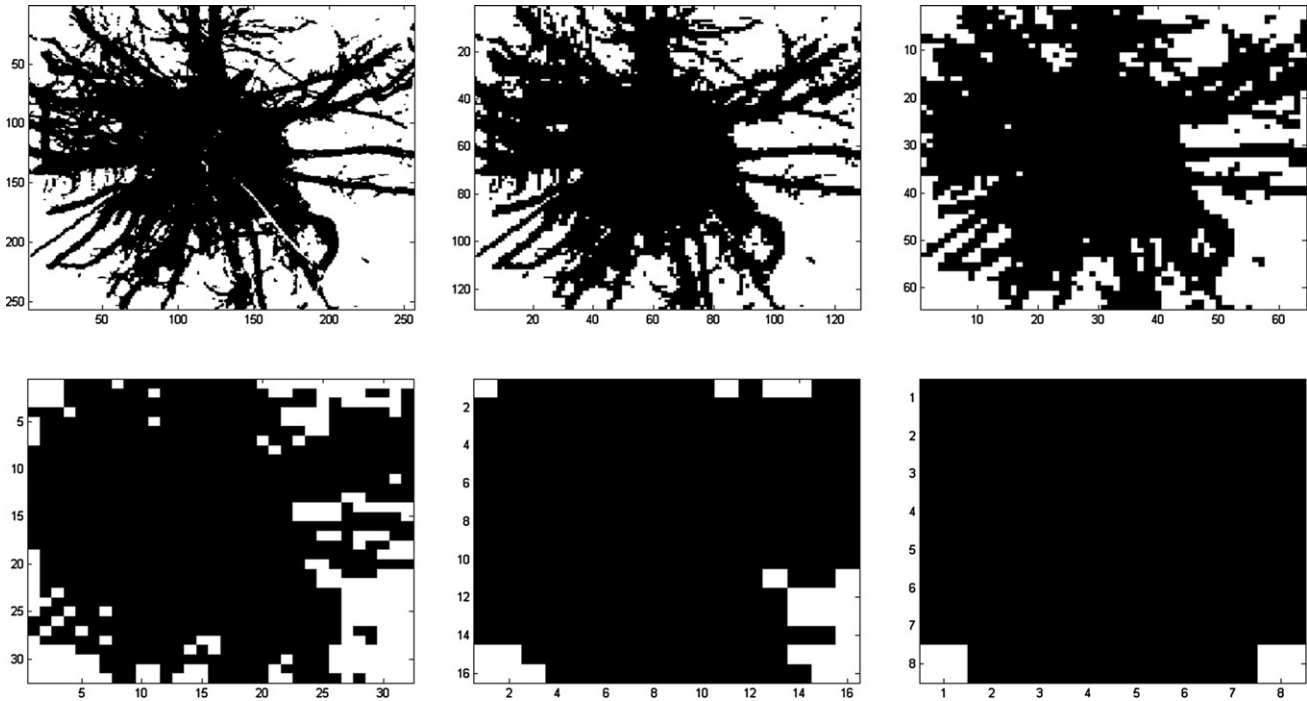


Fig. 3 – The images shown represent the process of calculating the Fractal Dimension of a root (here using a top view image). The grid size was gradually reduced from  $256 \times 256$  pixels (top left) to  $8 \times 8$  pixels (bottom right). In each image, the number of pixels that intercept with the root was counted. This led to six data points that served to calculate the Fractal Dimension.

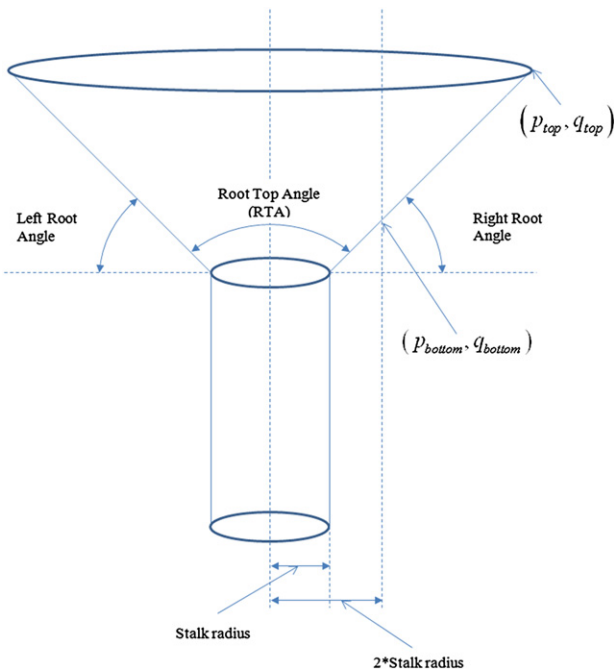


Fig. 4 – A simple topological model of a maize Root (presented upside down) is formed by a vertical cylinder that represents the stalk, and a cone shape that represents the root mass. The challenge is to find the starting point of the cylinder at the bottom, the transition from the cylinder to the cone, and the “rim” of the cone.

The  $(p_{bottom}, q_{bottom})$  coordinate, as shown in Fig. 4, is impossible to define in an absolute sense for a real maize root, since the transition point between the stalk (represented by the cylinder) and the root volume (represented by the cone) is not uniquely identifiable. Fortunately, the Left and Right Root Angles are not highly sensitive to the choice of  $p_{bottom}$ , and therefore, an arbitrary measure was used: the root section was assumed to start at the point where the accumulated pixel value is larger than or equal to twice the stalk radius. The constant two is the only arbitrary value in the procedure, and choosing this value rather large avoided problems with nodes protruding from the stalk such as is the case in the root shown in Fig. 2. In addition, since the choice of  $p_{bottom}$  is arbitrary, the method is robust against errors in the stalk diameter measurement which sometimes occurred owing to the presence of brace roots in the images. In Fig. 5, on the left hand side  $(p_{top}, q_{top})=(406,483), (p_{bottom}, q_{bottom})=(139,262)$  resulting in a Left Root Angle of  $39.6^\circ$ . On the right hand side  $(p_{top}, q_{top})=(475,598), (p_{bottom}, q_{bottom})=(123,298)$ , resulting in a Right Root Angle of  $40.4^\circ$ . The RTA was therefore  $100.0^\circ$ .

Fig. 6 shows an image in which the original root is overlaid with the stalk diameter (vertical straight lines) as well as the Left and Right Root Angles (slanted lines). Although there is no standard to compare to, it is clear that the Left and Right Root Angles are in agreement with the overall root shape.

#### 2.4. Data analysis

Data sets containing FD and RTA measurements of roots obtained from Illinois ( $N_{Root} = 1143$ ) and Missouri ( $N_{Root} = 789$ )

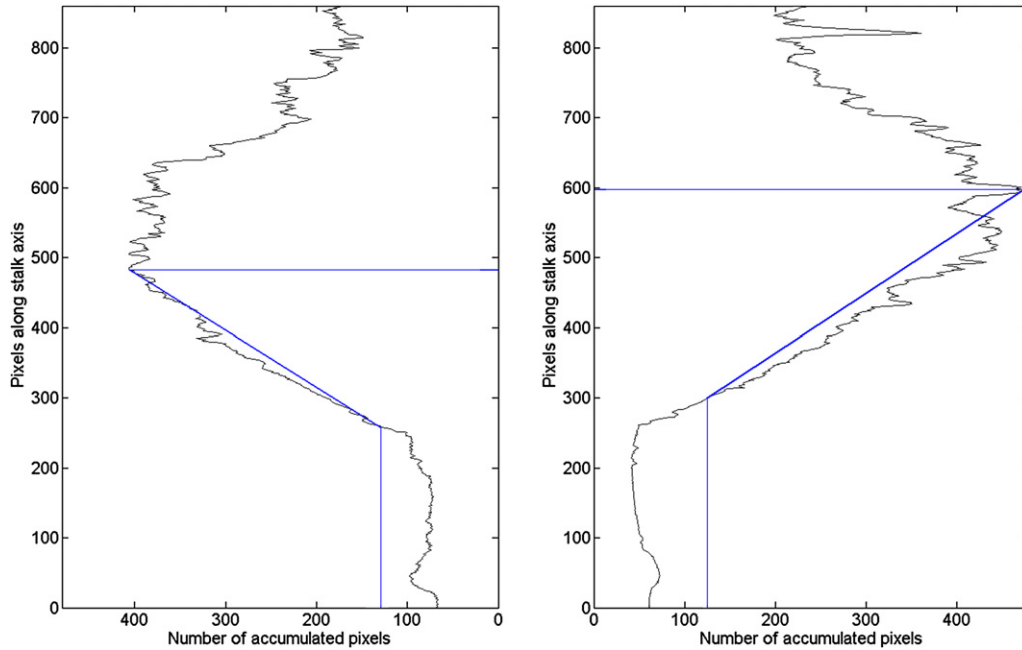


**Fig. 5 – Accumulated pixels of the root as shown in the bottom right image of Fig. 2. The accumulated pixels give a measure of the root “mass”. The “rim” of the cone ( $p_{top}, q_{top}$ ) was taken as the maximum value of the accumulated pixels. The transition from the cylinder to the cone ( $p_{bottom}, q_{bottom}$ ) was taken as the point where the number of accumulated pixels equalled twice the stalk radius.**

were combined. Plot means were calculated and an analysis of variance (ANOVA) procedure was followed to detect significant differences among recombinant inbred lines. The mixed model applied was:

$$y_{ijk} = \mu + \alpha_i + \beta_{(ij)} + g_k + \epsilon_{(ijk)} \quad (1)$$

where  $y_{ijk}$  represents the phenotypic plot mean of an entry,  $\alpha_i$  is the random effect of the  $i^{th}$  replication,  $\beta_{(ij)}$  is the random effect of the  $j^{th}$  block within the  $i^{th}$  replication,  $g_k$  is the fixed

effect of the  $k^{th}$  genotype, and  $\epsilon_{ijk}$  represents the residual error,  $NID(0, \sigma^2)$ . Marginal means were estimated for each genotype. Phenotypic correlation coefficients among traits were calculated from the marginal mean values of each trait applying standard methods (Mode & Robinson, 1959). All analyses were performed using SAS statistical software 9.1 (SAS Institute, 2003).

### 3. Results and discussion

The performance of the phenotyping method was assessed by a statistical analysis using 1932 roots. For each root system, five images from different views of the root were taken, i.e., one image from the top view (F0, see the bottom left subplot in Fig. 2) and four images from lateral views (S0 (see the bottom right subplot in Fig. 2), S90, S180, S270). If the assumption that roots are fractal-like objects holds true, FD values obtained from the different views of a root system must be correlated. Correlation coefficients were determined using marginal means of FDs for all 200 testcrossed recombinant inbred lines. All correlation coefficients were highly significant ( $P < 0.001$ ) and ranged from 0.77 to 0.83 between FD values obtained from lateral and top images combined, and from 0.83 to 0.88 for FD values determined for lateral images only. The fact that strong associations were observed between FDs for lateral and top images was unexpected (Fig. 7A shows the relationship between FD means for views F0 and S0). Given the assumption that roots are self-similar objects, finding significant correlations was expected, but since the images exhibit dramatic differences, one being quasi point-symmetric without a stalk, the other being quasi line-symmetric with a stalk, a much

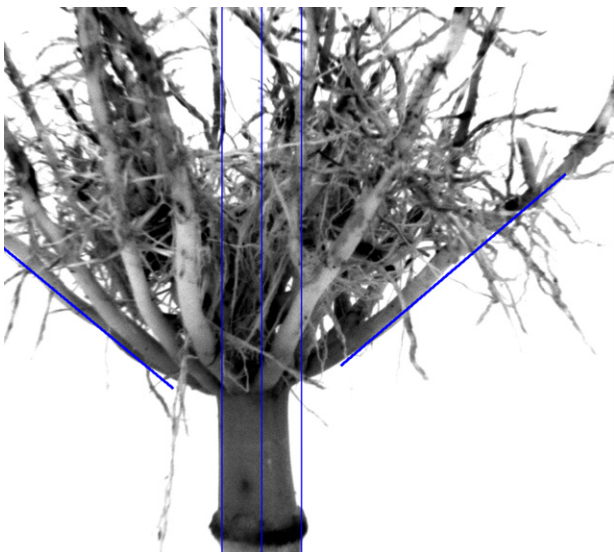


**Fig. 6 – Image of a maize root with the Left and Right Root Angle overlaid.**

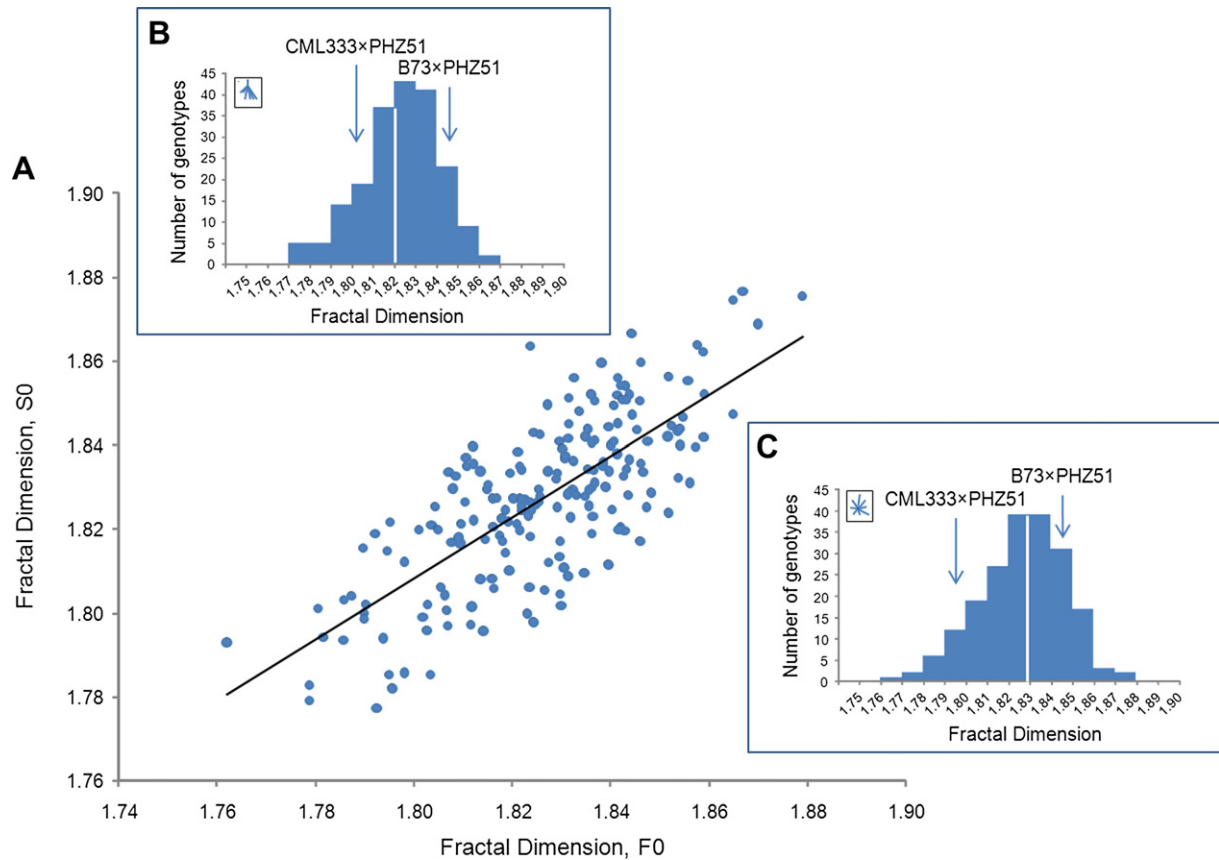


**Fig. 7 – A.** The relationship between mean fractal dimension (FD) values of roots. For each root system the FD was determined using a top view image (F0) and a side view image (S0), respectively. The linear relationship between F0 and S0 is explained by the regression model  $y = 0.73x + 0.50$  which explains 56% of the phenotypic variation for these traits in the population B73 × CML333. **B.** and **C.** are histograms for the mean FD of maize roots among 200 testcrossed recombinant inbred lines derived from cross B73 × CML333 based on their vertical ( $\bar{x}=1.82$ ,  $SE=0.017$ ) and horizontal view images ( $\bar{x}=1.83$ ,  $SE=0.019$ ). For both views, the FDs were highly significant ( $P < 0.0005$ ) among the recombinant inbred lines. Note that the white vertical lines in the histograms indicate the means.

lower correlation was expected. These results provide circumstantial evidence that roots are indeed fractal-like structures.

Insets B and C show histograms of the FDs of the lateral images (B) and the top images (C). Highly significant ( $P < 0.001$ ) differences between recombinant inbred lines were detected for FDs based on lateral and top images. Parental testcrosses B73 × PHZ51 and CML333 × PHZ51 differed significantly ( $P < 0.01$ ) with respect to their FDs. Transgressive segregation of FD in both image views was observed. As suggested by the tight correlation between FDs for lateral and top views, the histograms were very similar with respect to their population mean FDs ( $FD_{lateral}=1.82$ ;  $FD_{top}=1.83$ ) and observed variances.

Fig. 8 shows the distribution of RTA means among the 200 testcrossed recombinant inbred lines and their testcrossed parents B73 and CML333. RTAs ranged from 52 to 88° with a population mean of 70°. RTA differences among recombinant inbred line testcrosses and between both parental testcrosses were highly significant ( $P < 0.001$ ). The analysis of variance revealed highly significant ( $P < 0.001$ ) differences among recombinant inbreds. Based on previous information, inbreds B73 and CML333 were expected to exhibit dramatically

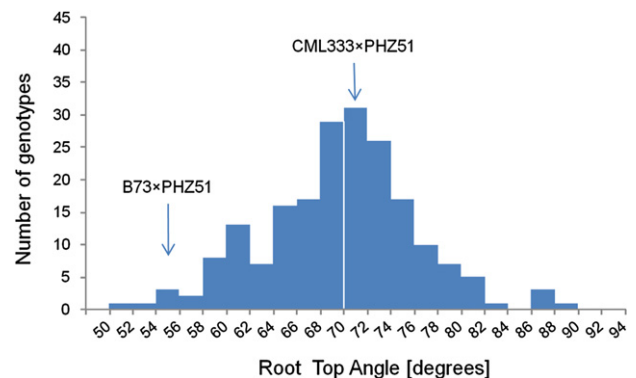


**Fig. 8 – Histogram of the Root Top Angle (RTA) of lateral root images from a dataset of 1932 images. The RTA population mean is 69.7 and its standard error is 6.57. Differences among recombinant inbred lines for RTA were highly significant ( $P < 0.0037$ ).**

different root angles, since B73 is a “narrow angled” inbred with an upright leaf and tassel posture and small RTAs and, in contrast, CML333 is characterised by larger leaf angles, tassel angles, and RTAs.

In addition to their testcrosses, B73, CML333, and tester PHZ51 were evaluated as inbreds with regard to their FDs and RTAs (data not shown). Initial evidence showed that root complexity is a maize phenotype probably determined by a multitude of genes with small effects. In addition, testcrosses showed significant hybrid vigour for root complexity. Combining FD and RTA data from both the testcross and inbreds *per se*, first hypotheses about the inheritance of root complexity and root angle in maize were derived and tested. If genes involved in the expression of root complexity (represented by FD) and RTA are acting in an additive mode, it is expected that the phenotype of a hybrid, which was derived by crossing two inbreds, would not be significantly different from the mean phenotype of these parental inbreds. This was the case in evaluation of the RTAs: parental testcross hybrid RTAs did not significantly differ from the average RTA of the two inbreds crossed to produce the hybrid, *e.g.*:

$$\begin{aligned} \text{Contrast}_1 &= \frac{RTA_{B73} + RTA_{PHZ51}}{2} - RTA_{B73 \times PHZ51} = 1.00\text{deg} \\ \text{Contrast}_2 &= \frac{RTA_{CML333} + RTA_{PHZ51}}{2} - RTA_{CML333 \times PHZ51} = 0.65\text{deg} \end{aligned} \quad (2)$$

Neither contrast was significantly different from zero, which is in agreement with the assumption that RTA is additively inherited.

For FD and RTA, substantial transgressive segregation was observed, *i.e.*, a number of recombinant inbred lines showed more extreme root phenotypes than their parents. These results are commonly observed in breeding experiments indicating that both parental inbreds carry genes that increase as well as decrease the trait under study (Balint-Kurti *et al.*, 2007; Rieseberg, Archer, & Wayne, 1999). Recombining both parental genomes produces recombinant inbreds that contain more positively or negatively acting alleles than either parents. As a consequence, these recombinant inbreds display extreme genotypes as seen in the root complexity experiment.

Another interesting finding was that the FD and RTA estimates were not significantly correlated among recombinant inbred lines. Therefore, it can be speculated that FD and RTA describe independent aspects of what constitutes root architecture and that, in the maize plant, both traits are controlled and respond independently to various abiotic and biotic stresses.

#### 4. Conclusions

Two phenotypical maize root characteristics were measured using a dedicated imaging system along with analysis software. The phenotypical characteristics were Fractal Dimension (FD) as a proxy for root complexity and the Root Top Angle (RTA).

The measurement arrangement was capable of producing high quality information that was highly repeatable: highly significant genotypic variances were observed in a population

of maize recombinant inbred lines for both FD and RTA. This is a key prerequisite for improving maize root characteristics to meet future challenges in maize production that could not yet be adequately addressed owing to a lack of appropriate high-throughput methods. The development and validation of the technologies as presented here could only be achieved through synergistic collaboration between an Engineering Department and a Crop Sciences Department.

#### Acknowledgements

The authors would like to express their appreciation to all students from the University of Illinois that assisted in the root data collection process. We also appreciate the collaboration with Dr. Sherry Flint-Garcia and Dr. Bruce Hibbard, USDA-ARS, Columbia, Missouri. Funding for this project was provided by Pioneer Hi-Bred® and the college of Agricultural Consumer and Environmental Sciences (ACES) of the University of Illinois.

#### REFERENCES

- Abraham, E. R. (2001). The fractal branching of an arborescent sponge. *Marine Biology*, 138, 503–510.
- Arsenault, J. L., Poulcur, S., Messier, C., & Guay, R. (1995). WinRHIZO, a root measuring system with a unique overlap correction method. *HortScience*, 30, 906.
- Balint-Kurti, P. J., Zwonitzer, J. C., Wissler, R. J., Carson, M. L., Oropeza-Rosas, M. A., Holland, J. B., *et al.* (2007). Precise Mapping of quantitative trait Loci for Resistance to Southern leaf Blight, caused by *Cochliobolus heterostrophus* Race O, and Flowering time using advanced Intercross maize lines. *Genetics*, 176, 645–657.
- Berntson, G. M. (1996). Fractal geometry, scaling and the description of plant root architecture. In Y. Waisel, A. Eshel, & U. Kafkafi (Eds.), *Plant roots: The hidden half* (pp. 259–272). New York: M. Dekker Inc.
- Box, J. E. (1996). Modern methods for root investigations. In Y. Waisel, A. Eshel, & U. Kafkafi (Eds.), *Plant roots: The hidden half* (pp. 193–237). New York: M. Dekker Inc.
- Bohn, M., Novais, J., Fonseca, R., Tuberosa, R., & Grift, T. E. (2006). Genetic evaluation of root complexity in maize. *Acta Agronomica Hungarica*, 54(3).
- Cunningham, M., Adams, M. B., Luxmoore, R. J., Post, W. M., & DeAngelis, D. L. (1989). Quick estimates of root length, using a video image analyzer. *Canadian Journal of Forest Research*, 19, 335–340.
- Eghball, B., Settimi, J. R., Maranville, J. W., & Parkhurst, A. M. (1993). Fractal analysis for morphological description of maize roots under nitrogen stress. *Agronomy Journal*, 85, 287–289.
- Eshel, A. (1998). On the fractal dimensions of a root system. *Plant, Cell and Environment*, 21, 247–251.
- Fernandez, E., Eldred, W. D., Ammermuller, J., Block, A., von Bloh, W., & Kolb, H. (1994). Complexity and scaling properties of amacrine, ganglion, horizontal, and bipolar cells in the turtle retina. *Journal of Comparative Neurology*, 15(347), 397–408, 3.
- Hammer, G. L., Dong, Z., McLean, G., Doherty, A., Messina, C., Schussler, J., *et al.* (2009). Can changes in canopy and/or root system architecture explain historical maize yield trends in the U.S. corn belt? *Crop Science*, 49(1), 299–312.

- Kaspar, T. C., & Ewing, R. P. (1997). ROOTEDGE: software for measuring root length from desktop scanner images. *Agronomy Journal*, 89, 932–940.
- Kubler, J. E., & Dugeon, S. R. (1996). Temperature dependent changes in the complexity of form of *Chondrus crispus* fronds. *Journal of Experimental Marine Biology and Ecology*, 207, 15–24.
- Lontoc-Roy, M., Dutilleul, P., Prasher, S. O., Han, L., Brouillet, T., & Smith, D. L. (2006). Advances in the acquisition and analysis of CT scan data to isolate a crop root system from the soil medium and quantify root system complexity in 3-D space. *Geoderma*, 137, 231–241.
- Lynch, J., Johannes, J., & Beem, V. (1993). Crop physiology and metabolism: growth and architecture of seedling roots of common bean genotypes. *Crop Science*, 33, 1253–1257.
- Lynch, J. (1995). Root architecture and plant productivity. *Plant Physiology*, 109, 7–13.
- Mandelbrot, B. B. (1983). *The fractal geometry of nature*. New York: Freeman.
- Masi, C. E. A., & Maranville, J. W. (1998). Evaluation of sorghum root branching using fractals. *The Journal of Agricultural Science Cambridge*, 131, 259–265.
- Mihail, J. D., Obert, M., Bruhn, J. N., & Taylor, S. J. (1995). Fractal geometry of diffuse mycelia and rhizomorphs of *Armillaria* species. *Mycological Research*, 99, 81–88.
- Mode, C. J., & Robinson, H. F. (1959). Pleiotropism and genetic variance and covariance. *Biometrics*, 15, 518–537.
- Nielsen, K. L., & Lynch, J. (1994). Fractal analysis of bean root systems. *Agronomy Abstracts*, 150.
- Oppelt, A., Kurth, W., Dzierzon, H., Jentschke, G., & Godbold, D. (2000). Structure and fractal dimensions of root systems of four co-occurring fruit tree species from Botswana. *Annals of Forest Science*, 57, 463–475.
- Ottman, M. S., & Timm, H. (1984). Measurement of viable plant roots with the image analysing computer. *Agronomy Journal*, 76, 1018–1020.
- Richardson, A. D., & zu Dohna, H. (2003). Predicting root biomass from branching patterns of Douglas-fir root systems. *OIKOS*, 100, 96–104.
- Rieseberg, L. H., Archer, M. A., & Wayne, R. K. (1999). Transgressive segregation, adaptation and speciation. *Heredity*, 83, 363–372.
- SAS Institute. (2003). *SAS/STAT User's guide, Release 9.1 edn*. Cary: SAS.
- Soethe, N., Lehmann, J., & Engels, C. (2007). Root tapering between branching points should be included in fractal root system analysis. *Ecological Modelling*, 207, 363–366.
- Spek, L. Y., & Van Noordwijk, M. (1994). Proximal root diameters as predictors of total root system size for fractal branching models. II. Numerical model. *Plant and Soil*, 164, 119–128.
- Tatsumi, J., Yamauchi, A., & Kono, Y. (1989). Fractal analysis of plant root systems. *Annals of Botany*, 64, 499–503.
- Walk, T. C., Van Erp, E., & Lynch, J. P. (2004). Modelling applicability of fractal analysis to efficiency of soil exploration by roots. *Annals of Botany*, 94, 119–128.